

Article

Biosynthesis of Nano-Selenium and Its Impact on Germination of Wheat under Salt Stress for Sustainable Production

Azza A. Ghazi ^{1,*}, Sahar El-Nahrawy ¹, Hassan El-Ramady ²  and Wanting Ling ^{3,*}

¹ Agriculture Microbiology Department, Soils, Water and Environment Research Institute (SWERI), Sakha Agricultural Research Station, Agriculture Research Center (ARC), Kafrelsheikh 33717, Egypt; sahar.elnahrawy@yahoo.com

² Soil and Water Department, Faculty of Agriculture, Kafrelsheikh University, Kafrelsheikh 33516, Egypt; hassan.elramady@agr.kfs.edu.eg

³ Institute of Organic Contaminant Control and Soil Remediation, College of Resource and Environmental Sciences, Nanjing Agricultural University, Nanjing 210095, China

* Correspondence: ghaziazza@yahoo.com (A.A.G.); lingwanting@njau.edu.cn (W.L.)

Abstract: Selenium and its derivatives have been found capable of excellent biological responses. However, the element in its bulk form has low bioavailability and increased toxicity, meaning the production of effective forms with sustainable methods has become urgent. Several microorganisms, including fungi, bacteria and yeast, as well as higher plants, are capable of biosynthesizing nanoparticles such as nano-selenium (nano-Se), which has wide applications in medicine, agriculture and industry. Thus, the biosynthesis of nano-Se using some bacterial species was the main target of this study. The production of nano-Se and the monitoring of its impact on the wheat germination of seeds under salt stress (i.e., 50, 100, and 150 mM NaCl) was also evaluated in the current study. The ameliorative role of nano-Se doses (i.e., 50, 75, and 100 mg L⁻¹) in the germination of wheat seeds under salt stress was also investigated. Based on sodium selenite tolerance and reducing selenite to elemental Se-NPs, the most effective isolate (TAH) was selected for identification using the 16S rRNA gene sequence, which belonged to *Bacillus cereus* TAH. The final germination percent, mean germination time, vigor index and germination rate index were improved by 25, 25, 39.4 and 11%, respectively, under 15 mM sodium chloride concentration when 100 mg L⁻¹ nano-selenium was used. On the other hand, the results obtained from a gnotobiotic sand system reveal that with treatment with 100 mg L⁻¹ nano-selenium under high Ec values of 14 ds m⁻¹, the vegetative growth parameters of shoot length, root length, fresh weight and dry weight were improved by 22.8, 24.9, 19.2 and 20%, respectively, over untreated controls. The data obtained from this study reveal that the use of nano-selenium produced by *Bacillus cereus* offers improved wheat seed germination under a salt-affected environment.

Keywords: screening; identification; human health; biological nanoparticles; *Bacillus cereus*



Citation: Ghazi, A.A.; El-Nahrawy, S.; El-Ramady, H.; Ling, W. Biosynthesis of Nano-Selenium and Its Impact on Germination of Wheat under Salt Stress for Sustainable Production. *Sustainability* **2022**, *14*, 1784. <https://doi.org/10.3390/su14031784>

Academic Editor: Svein Øivind Solberg

Received: 30 December 2021

Accepted: 27 January 2022

Published: 4 February 2022

Publisher's Note: MDPI stays neutral with regard to jurisdictional claims in published maps and institutional affiliations.



Copyright: © 2022 by the authors. Licensee MDPI, Basel, Switzerland. This article is an open access article distributed under the terms and conditions of the Creative Commons Attribution (CC BY) license (<https://creativecommons.org/licenses/by/4.0/>).

1. Introduction

There is a growing demand for literature that identifies the importance of nanotechnology in our lives nowadays. This science has great applications in medicine, agriculture, industry and many other emerging fields [1]. Nanotechnology could be defined as an interdisciplinary science that includes the production or synthesis of nanomaterials (1–100 nm) and their applications in different fields [2]. These nanomaterials or nanoparticles have distinguished shapes and sizes, as well as unique magnetic, optical, chemical, electrical and mechanical properties, compared to their bulk counterparts [3]. One could produce these nanoparticles using physical, chemical and biological methods, and the biological ways are still the most desirable approaches [4] due to their advantages, including the nature of these nanoparticles being non-toxic, clean and environment-friendly [5]. Many biological sources could be used to produce nanoparticles, such as bacteria, plant extracts,

actinomycetes, yeast, viruses, fungi and algae [1]. The nanoparticle biosynthesis of metal oxides (e.g., CuO, CeO₂, Fe₃O₄, TiO₂, and ZnO), metals (e.g., Ag, Mn and Cu) or metalloids (e.g., Se and Si) has been reported in several applications [6], such as removing pollutants from wastewater [7], agriculture [8], and biomedicine [9].

Selenium (Se) was, and still is, one of the most important elements, which humans, animals and lower plants cannot live without, and the nanoparticles of this nutrient (nano-Se) have promising applications [10,11]. The biosynthesis of nano-Se using different sources, such as plant extracts [12–14], fungi [15] and bacteria [16], has been reported by many researchers. Nano-Se has been used in therapeutic [11,17] and nano-medicine applications [10,18] for humans and animals, as well as in cancer gene and drug delivery [19,20]. In agriculture, the remediation of contaminated soils with pollutants could be achieved using nano-Se, such as removing mercury [21]. Several species of bacteria have been successfully used to biosynthesize selenium nanoparticles, such as *Pseudomonas putida* KT2440 [22], *Rhodococcus aetherivorans* BCP1 [16], *Acinetobacter* sp. SW 30 [23], *Enterococcus faecalis* [24], *Azoarcus* sp. CIB [25], *Stenotrophomonas maltophilia* SeITE02 [26], *Azospirillum thiophilum* [27], *Staphylococcus aureus* [28] and *Bacillus cereus* [29].

Seed germination in wheat plants is considered the most critical period in plant life due to its potential effect on the quantity and quality of grain yield [30,31]. The germination of wheat seeds and its mechanisms still require more explanation [32], particularly when under environmental stresses, which may increase reactive oxygen species and decline the uptake of nutrients and water deficit [33]. As reported in some studies, selenium has exhibited a prominent role in protecting wheat seeds and seedlings against salt stress [34]. It could be applied to many biostimulators to enhance the germination of cultivated seeds under stressful environments, such as nanoparticles [2]. Priming wheat seeds with potassium silicate, ascorbic acid, and proline could also alleviate salinity stress during their germination [35]. Many studies have been carried out, including on the role of nanoparticles in promoting seed germination under stresses, such as silica nanoparticles under salt stress conditions in common bean and cucumber [36,37] and fenugreek [38], as well as using nano-Se under conditions of high-temperature stress in sorghum [39], and nano-ZnO under drought stress conditions in sorghum [40], but very few studies have been carried out concerning the impact of nano-Se on wheat seed germination under salt stress conditions [41].

It was found that the conversion of inorganic forms of selenium into nanoforms significantly reduces its toxicity. Chemical synthesis methods of nano-selenium suffer from several disadvantages, such as the use of several additives for controlling particle morphology, multistage synthesis, and high production costs, in addition to environmental toxicity. Biological synthesis using microorganisms (algae, fungi, yeast, bacteria) is a sustainable, environment-friendly, and cost-effective approach.

The efficacy of biosynthesized nano-selenium has been demonstrated in many fields, but there are few research papers that discuss its validity and distinction in the field of plant nutrition. The current study contributes to knowing the extent of the possibility of using biosynthetic nano-selenium to support plant growth under unfavorable conditions.

Therefore, the main target of this study is to investigate the biosynthesis of nano-Se and its role in improving the germination of wheat seeds. The isolation, screening and identification of nano-Se mediated by *Bacillus cereus* have also been highlighted.

2. Materials and Methods

The sequence of work in the current study was summarized in the following flowchart Figure 1.

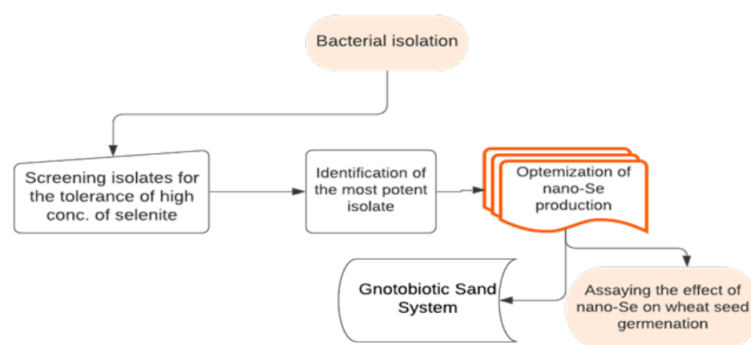


Figure 1. A flow chart describing the main steps of the current study.

2.1. Isolation and Characterization of Bacteria Transforming Selenium

The isolates were obtained from soil samples collected from Sakha Agricultural Research Station experimental farm, Kfr ElSheikh, Egypt, according to standard procedures [42]. The most potent isolate was selected based on its potential to tolerate high concentrations of selenium as selenite (SeO_3^{2-}). The screening of isolates for selenite tolerance was conducted in tryptone soy broth (TSB), amended with Na_2SeO_3 (300 mg L^{-1}). The morphological and Gram-staining characterization of selected isolates were carried out according to standard protocols [43].

2.2. Nano-Selenium Production

Nutrient broth medium was prepared, after autoclaving for 20 min at 121°C , then a sterilized sodium hydrogen selenite (NaHSeO_3) solution was supplemented from a $10,000 \text{ mg/L}$ stock solution to reach 300 mg L^{-1} concentration. The flasks were inoculated with a 10% inoculum of 24 h-old *Bacillus cereus* strain culture before incubating for 48 h in an orbital shaker at 200 rpm and 30°C . At the end of the incubation time, the culture medium color turned to red, indicating the synthesis of nano-selenium. The fermentation broth was centrifuged for 20 min at 5000 rpm and the supernatant was discarded. The remaining bacterial pellets were washed 3 successive times with 0.9% NaCl solution, then treated with 37% HCl, kept for 2 days at room temperature, and then centrifuged and washed several times using distilled water to remove HCl. The obtained red precipitate was dried at 70°C and used for further investigation.

2.3. Scanning Electron Microscope (SEM) Analysis

A high-resolution SEM (HR-TEM, Tecnai G20, FEI, Eindhoven, The Netherlands) was used for identifying the size and shape of the synthesized nano-selenium particles. Two different imaging modes were used—bright field (electron accelerating voltage 200 kV, LaB6 as electron source gun) and diffraction pattern imaging (DPI). An eagle CCD camera with a $4 \text{ k} \times 4 \text{ k}$ resolution was used to collect transmitted electron images. TEM Imaging & Analysis software was used to analyze the spectrum of EDX peaks.

2.4. UV Spectroscopic Analysis

Absorption spectra of the synthesized nano-selenium were obtained using a UV–VIS spectrophotometer, Jenway, Model 6705 at a wavelength range of 200–800 nm.

2.5. Molecular (16S) Identification of Selected Isolate

The genomic DNA of bacterial biomass was isolated with a Gene Jet Kit (Fermentas). Then 16S rRNA genes were amplified via PCR (a hybrid thermocycler and the Maxima Hot Start PCR Master Mix) using universal forward and reverse primers (F, 5'-AGA GTT TGA TCC TGG CTC AG- '3 and R, 5'-GGT TAC CTT GTT ACG ACT T-3'). The resulting amplified products were eluted in agarose gel, and the 16S rRNA gene was sequenced using an ABI 3730xl DNA Sequencer at GATC Biotech DNA Sequencing, Constance, Germany.

Data were analyzed using the BioEdit software 5.0.9 sequence editor. The sequence was aligned by the RDP Sequence Aligner software (<https://rdp.cme.msu.edu/>, accessed on 21 December 2021). A dendrogram and the tree topology were constructed using the method of neighbor-joining. The bacterial isolate was identified as *Bacillus cereus* TAH, and the sequence of the 16S rRNA gene was deposited in a gene bank with the accession number MW676031.

2.6. Effect of Selenite Concentration on Synthesis of Selenium Nanoparticles

The role of selenite concentration (1.0–10 mM) on nanoparticle production was assayed in nutrient broth medium incubated under shaking at 150 rpm and 30 °C for 72 h. The cell billets and nanoparticles were obtained by centrifugation at 10,000 × *g* for 10 min, and then the residual selenite concentration in the supernatants was quantified using atomic absorption (Perkin Elmer pin AAcle 500, Waltham, MA, USA).

2.7. Effect of Incubation Conditions (Static or Shaking) on Nano-Se Production

Selenite reduction was carried out in an 250 mL Erlenmeyer flask containing 100 mL of nutrient broth containing 8 mM sodium selenite. The flasks were incubated at 30 °C for 72 h under static or shaking conditions at a shaking speed of 150 rpm. The samples were then centrifuged at 10,000 × *g* for 10 min. Selenium was measured in the supernatant, as mentioned previously.

2.8. Testing the Synthesis of Nano-Selenium Using Washed Cells of *B. cereus* TAH or Culture Supernatant

The nutrient broth was inoculated with 10% of a 24 h-old culture of *B. cereus* TAH, then incubated for 48 h at 30 °C and a 150 rpm shaking speed. After incubation, cells were harvested through centrifugation at 10,000 × *g* for 10 min. Afterward, the supernatant was sterilized using a 0.22 μm membrane filter, and the cells pellets were washed with phosphate buffer pH = 7 and resuspended in the same buffer and the same volume of original culture in a sterile Erlenmeyer flask. Both supernatant and cell suspension were supplemented with 8 mM sodium selenite and incubated for 48 h at 30 °C and 150 rpm. Another group was heated to 121 °C for 15 min in Autoclave. Phosphate buffer and nutrient broth supplemented with 8 mM sodium selenite were used as controls in both groups. The formation of nano-selenium was identified by the development of a red color, and the production percent was measured by quantifying selenium in the supernatant.

2.9. Effect of Nano-Selenium on Wheat Seed Germination

The experiment was carried out to examine the potential abilities of different nano-Se concentrations (0, 50, 75, and 100 mg L⁻¹) to enrich the seed germination of sensitive wheat cultivars (Sids 1) under elevated NaCl stress (50, 100, and 150 mM). For this purpose, 10 seeds were first washed with 70% ethanol then surface-sterilized for 3 min with a 5% solution of sodium hypochlorite, and then residues of hypochlorite were removed by washing five times with sterile distilled water and spread in petri dishes lined with sterilized filter paper. Next, 10 mL of salt solution supplemented with one of the above nano-Se concentrations was add to each petri plates and left to germinate for 10 days in a dark incubator at 25 °C. The plates were sealed with polyethylene sheets to keep a constant moisture level during the germination period. The germinated seeds were enumerated daily and germination parameters were assayed as follows.

- a. Final germination %

$$\text{FGP}\% = \left[\frac{\text{TNG}}{\text{TNP}} \right] \times 100 \quad (1)$$

where FGP % refers to the final germination percentage, TNG refers to the total number of germinated seeds, and TNP refers to the total number of seeds [44].

- b. Mean germination time (MGT), calculated according to the formula:

$$\text{MGT} = \sum \left(\frac{n_i \times t_i}{n_i} \right) \quad (2)$$

where MGT refers to mean germination time, n_i refers to the number of germinated seeds on germination days, and t_i refers to the number of days during the germination interval (between 0 and 10 days) [45].

c. The vigor index (VI) was assayed according to Kharb et al., (1994) [46].

$$\text{VI} = \left[\frac{\text{SDM}(\text{g}) \times \text{GP}}{100} \right] \quad (3)$$

where VI = vigor index, SDM is the dry seedling mass (g), and GP = germination (%).

d. The germination rate index (GRI) was conducted according to the formula of Esechie (1994) [47], as follows:

$$\text{GRI} = \frac{G1}{1} + \frac{G2}{2} + \frac{GX}{X2} \quad (4)$$

where G1 refers to germination percentage at the first day after incubation; G2 refers to the germination percentage at the second day after germination; GX refers to the germination percentage at day x after incubation.

2.10. Gnotobiotic Sand System

This experiment was conducted in glass tubes with a dimensions of 2.5 cm diameter and 20 cm length to study the effects of different nano-Se concentrations (0, 50, 75, and 100 mg L⁻¹) on some growth dynamics of the wheat cultivar (Sids 1) exposed to different salinity stresses (7, 10 and 14 dS m⁻¹), with 5 replicates ($N = 5$).

Each tube received 50 g of a sterilized sand and vermiculite (1:1) mixture and 6 mL of sterilized Jensen's nutrient solution [48], supplemented with graduated salinity concentrations of seawater diluted to the equivalent of the above-mentioned salinity levels. Sterilized wheat seeds were soaked in different concentrations of nano-Se for 30 min and placed in sterile tubes, where each tube received one seed, and control seeds were soaked in distilled water. The tubes were incubated in a growth chamber with a photoperiod of 16:8 h at 20 °C. After 30 days, the lengths of shoots and roots and the fresh and dry weights of the plants were estimated.

2.11. Statistical Analyses

Using one-way analysis of variances (ANOVA), data were analyzed via SPSS software version 14.0 in relation to the Duncan's multiple range test, which was used for comparisons among the treatment means [49].

3. Results

3.1. Biosynthesis and Characterization of Selenium Nanoparticles

In the current study, 25 selenite-resistant bacterial isolates were screened for the production of Se-NPs by reducing selenite to red elemental selenium. The red color of the colonies on the solid culture is proof of the reduction of selenite to red elemental selenium, which could be observed, and this indicated this reduction of SeO₃⁻² to red Se⁰. The isolate TAH was the most efficient compared to other isolates (Figure 2a).

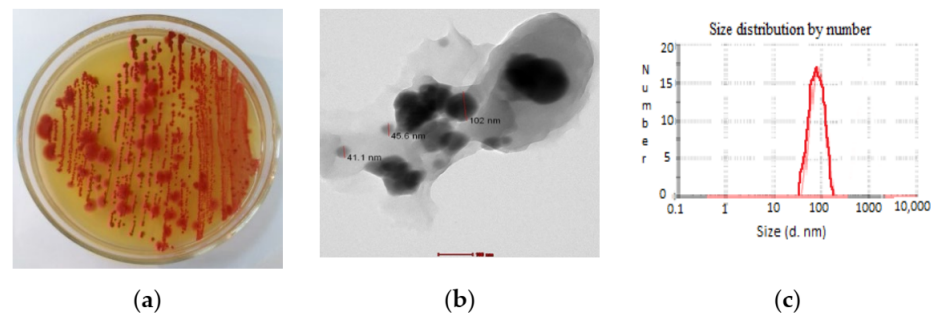


Figure 2. (a) *Bacillus cereus* TAH grown on nutrient agar supplemented with sodium selenite. (b) Scanning electron microscope image for the synthesized nano-selenium. (c) Particle size distribution for synthesized nano-selenium.

3.2. Transmission Electron Microscopic and Particle Size Distribution Analysis of SeNPs

The Transmission Electron Microscopy (TEM) images indicated the production of spherical SeNPs with a particle size between 41 and 102 nm (Figure 2b).

3.3. UV Spectroscopic Analysis

As shown in Figure 3, a good distinct absorption peak was detected in the UV region between 190 and 370 nm in the spectrum of synthesized nano-Se, displaying its nano-nature. The absorption spectrum remained constant over time, indicating the stability of the particles.

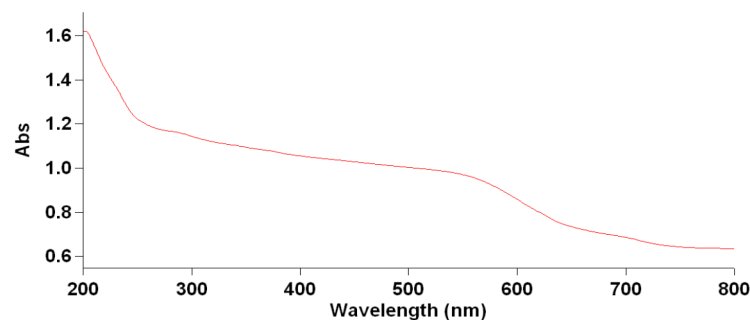


Figure 3. Absorption spectrum curve of nano-Se synthesized by *Bacillus cereus* TAH.

3.4. Identification of the Most Promising Bacterial Isolate

In the current work, 25 selenite-resistant bacterial isolates were obtained from soil collected from the experimental farm of Sakha Agricultural Research Station, Kafr El-Sheikh, Egypt. Based on the tolerance of sodium selenite and the reduction of selenite to red Se-NPs, the most promising isolate (TAH) was selected for identification (Figure 4). It was identified as *B. cereus*.

3.5. Effect of Selenite Concentration on Synthesis of Selenium Nanoparticles

The selenite reduction potential of *B. cereus* TAH was assayed by measuring the residual selenium concentration in the supernatants at different selenite levels (Figure 5). At a lower concentration of 1.0 mM, only 17% of selenite reduction was achieved within 72 h. The percentage of production of nano-selenium was increased by increasing the concentration of selenite until it reached 84% at a concentration of 8 mM. Afterward, the percentage began to decrease at concentrations of 9 and 10 mM.

3.6. Effect of Incubation Conditions (Static or Shaking) on Nano-Se Production

The results show that the incubation under static conditions negatively affected the reduction of selenite compared to incubation under shaking conditions, which led to a

conversion percentage about 3 times that under static conditions; this can be attributed to the speed of reproduction and multiplication of bacterial cells under shaking conditions (Figures 6 and 7).

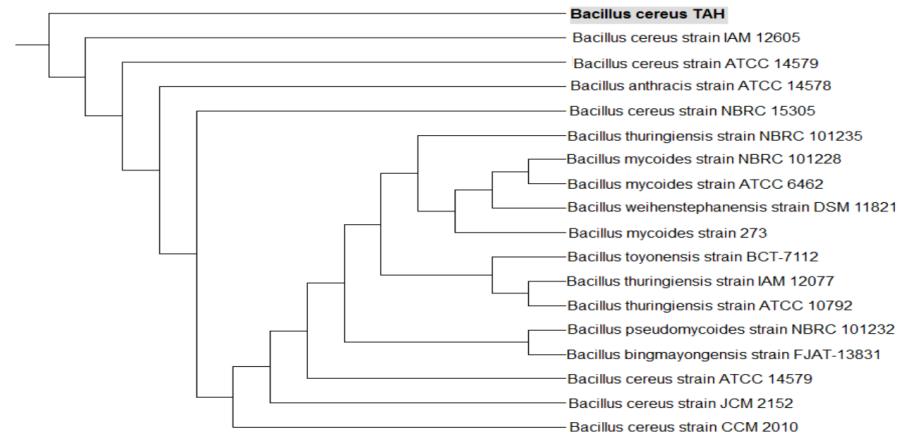


Figure 4. Dendrogram showing the phylogenetic tree of partial 16S rRNA gene sequences showing the position of the *Bacillus cereus* strain TAH 12 using 16S rRNA; the sequence was deposited in a gene bank under the accession number MW676031.

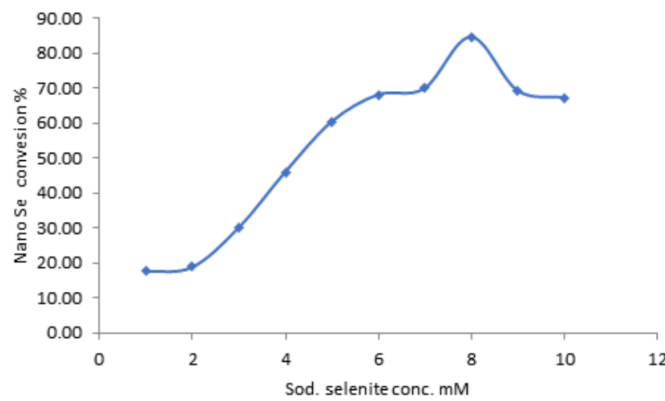


Figure 5. Effect of selenite concentration on nano-selenium production by *Bacillus cereus* TAH 12 in nutrient broth medium incubated under shaking at 30 °C for 72 h.

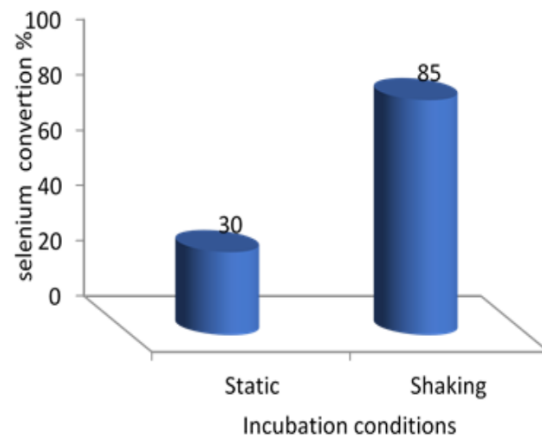


Figure 6. Effect of incubation conditions on the reduction of selenite to elemental nano-selenium.

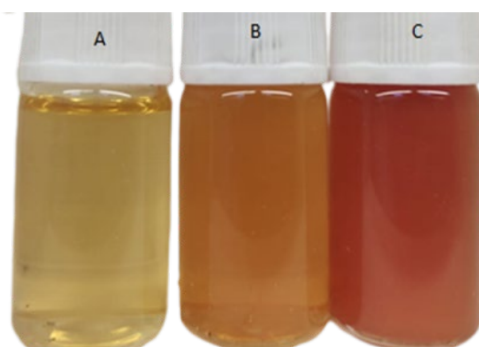


Figure 7. Effect of static or shaking conditions on the production of nano-Se by *Bacillus cereus* TAH. A: control; B: under static conditions; C: under shaking conditions.

3.7. Testing the Synthesis of Nano-Selenium Using Washed Cells of *B. cereus* TAH or Culture Supernatant

The ability of the washed *B. cereus* TAH cell or culture supernatant to reduce selenite to elemental selenium was examined. Neither the washed cells, the culture supernatant nor the control showed any activity in the reduction of selenite to selenium when incubated at 30 °C for 24 h. In comparison, the results were different under heat treatment at 121 °C for 15 min. The washed cells and supernatant, in addition to nutrient broth medium, were able to reduce selenite to selenium by 12, 7, and 10%, respectively (Table 1).

Table 1. Testing the synthesis of nano-selenium using washed cells of *B. cereus* TAH.

Treatments	Production Rate of Se ⁰ (%)
Control (buffer) at 30 °C	0.0
Control (buffer) at 121 °C	0.0
Cell pellets at 30 °C	0.0
Cell pellets at 121 °C	12
Control (nutrient broth) at 30 °C	1.0
Control (nutrient broth) at 121 °C	10
Supernatant at 30 °C	0.0
Supernatant at 121 °C	7.0

3.8. Germination of Wheat Seeds

The germination of wheat seeds was investigated under different dilutions of sea water as a source of salinity (Figure 8). Increasing salinity stress radically affected the final germination percent of wheat seeds (Figure 8a). Among all different concentrations of nano-Se, 75 mg L⁻¹ improved the final germination percent (FGP) under the highest level of salinity, which increased to 70 and 50% at 100 and 150 mM compared to the control (zero nano-Se), respectively.

On the other hand, all nano-Se concentrations showed a decreased MGT at high NaCl concentrations up to 150 mM (Figure 8b). The results showed that the shortest MGT was recorded for wheat seeds treated with 75 mg nano-Se L⁻¹ (4.5), followed by 100 mg nano-Se L⁻¹ (4.7), while the seeds of the control gave the longest MGT, reaching 5.4 at 150 mM NaCl. The vigor index (VI) values were intensely reduced at high salinity levels, particularly when the germination medium was supplemented with 150 mM NaCl. The application of 75 nano-Se L⁻¹ maximized the vigor index by 0.011 and 0.008 for 100 and 150 mM NaCl compared to the control (without nano-Se), respectively. The behavior of wheat seeds (as regards the germination rate index (GRI)) treated with different nano-Se concentrations under various levels of NaCl (Figure 8d) were as follows: increasing NaCl concentrations drastically decreased the GRI of wheat seeds treated with or without SeNPs, but an increase was observed in GRI at 150 mM for those seeds amended with 75 mg L⁻¹ Se-NPs, which attained 31.89% per day compared to other different concentrations of Se-NPs and control. A similar trend was noticed at 50 and 100 mM NaCl (Figure 8d).

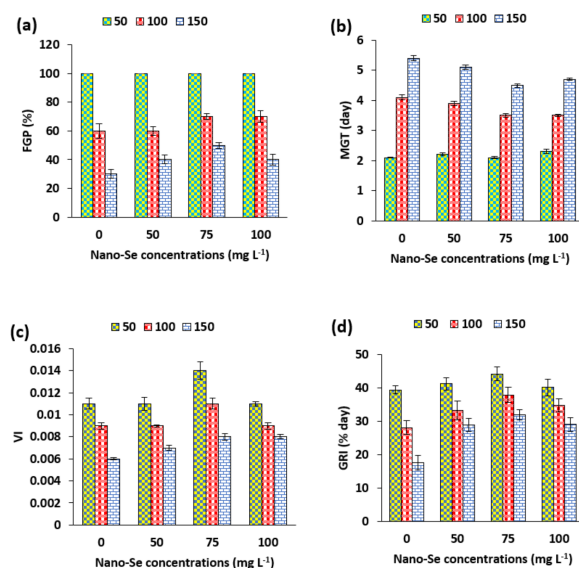


Figure 8. Effects of different concentrations of nano-Se on some different germination parameters of wheat seeds under varying levels of NaCl (50, 100 and 150 mM): (a) final germination percent, (b), mean germination time and (c), vigor index and (d) germination rate index.

3.9. Gnotobiotic Sand System

The responses of salinity-affected wheat cultivars (Sids 1) to different concentrations of nano-Se in a gnotobiotic system over one month are shown in Table 2. Generally, different concentrations of nano-Se increased the root and shoot length, as well as the fresh and dry weight, of wheat plants over the controls in a salt-stressed environment. The highly significant effect of shoot length at 50 mg L⁻¹ attained 18.5 cm plant⁻¹ at 7 dS m⁻¹, while at 14 dS m⁻¹, the shoot length recorded was 10 cm at 75 mg L⁻¹, compared to other nano-Se concentrations. For root length, the 100 mg L⁻¹ concentration showed a highly significant effect at 7, 10, and 14 dS m⁻¹, which reached 16.33, 17.66, and 14.66 cm plant⁻¹, respectively (Table 2). On the other hand, at 10 and 14 dS m⁻¹, the increases reached 50 and 52% for fresh weight (g plant⁻¹), and 66 and 75% for dry weight (g plant⁻¹), respectively.

Table 2. Effects of different concentrations of nano-Se on some growth dynamics of wheat plants under varying levels of salt stress (7, 10 and 14 dS m⁻¹).

Se Treatments (mg L ⁻¹)	Shoot Length (cm Plant ⁻¹)	Root Length (cm Plant ⁻¹)	Fresh Weight (g Plant ⁻¹)	Dry Weight (g Plant ⁻¹)
Salt stress at 7 dS m ⁻¹				
0	15.16 ab	12.33 de	0.033 d	0.007 abc
50	18.5 a	14.66 a–d	0.041 c	0.006 bc
75	17.33 ab	15.66 abc	0.045 b	0.010 ab
100	17.33 ab	16.33 ab	0.049 a	0.011 a
Salt stress at 10 dS m ⁻¹				
0	11.83 c	12.33 de	0.030 d	0.006 bc
50	14.83 b	15.33 a–d	0.037 c	0.008 abc
75	15.66 ab	16.66 ab	0.045 d	0.010 ab
100	16.66 ab	17.66 a	0.040 c	0.009 abc
Salt stress at 14 dS m ⁻¹				
0	7.33 d	11.00 e	0.021 f	0.004 c
50	9.83 cd	12.66 cde	0.026 e	0.005 bc
75	10.00 cd	14.33 bcd	0.032 d	0.007 abc
100	9.50 cd	14.66 a–d	0.026 e	0.005 bc
LSD (0.01)	2.57	2.25	0.003	0.003

In each column, means followed by a common letter are not significantly different at the 1% level, as assessed by Duncan's new multiple range test (DMRT).

4. Discussion

Transmission Electron Microscopy (TEM) is an appropriate high-resolution tool that offers actual information concerning the particle sizes and shapes of nanoparticles [50]. This technique is essential in characterizing materials from the atomic scale to hundreds of nanometers in size. The present data suggest the spherical form of the prepared SeNPs, which closely agrees with the results given by Kora et al. (2018) [29]. Particle size distribution analysis revealed that the biosynthesized SeNPs were ~ 100 nm (Figure 2c).

The inability of the washed cells and supernatant to reduce selenite at 30 °C indicates that the mechanism used in the reduction of selenium by *B. cereus* TAH is linked to the production of compounds that stimulate their production when selenite is present and are produced for the purpose of detoxification. The formation of nano-selenium when exposing the washed cell suspension to a high temperature indicates the presence of some structural compounds in the walls of these cells, rather than enzymes (such as selenite reductase), that can reduce selenite regardless of whether the cell is alive or not, as it behaves in this way as a chemical compounds (ascorbic acid, for example) that do this work. The reduction of selenite in a nutrient broth medium that is not inoculated with bacteria can be explained by this fact as well, since its components (peptone, beef extract and in some formulations yeast extract) are derived from animal or microbial cells. These results do not conform with the results stated by Kora et al. (2018) [29], who studied the localization of selenite reductase activity in a selenite-amended culture supernatant and the membrane protein fractions of *B. cereus* under normal temperatures, and found that selenite reduction was noted in both the membrane protein fraction and the supernatant. According to our results, the point of difference here is that *B. cereus* TAH does not produce proteins responsible for selenite reduction except in the presence of selenite.

The germination of any cultivated plant seeds is considered the critical stage of plant growth, in particular when under stress. Many studies have investigated the germination of wheat seeds under salt stress [51], as well as possible management approaches to overcome this stress, such as priming seeds with proline, ascorbic acid, potassium silicate, and spermidine [35]. Nanoparticles or nanomaterials have also been used successfully in the germination of wheat seeds, such as chitosan nanoparticles [52], ZnO nanoparticles [53] and iron oxide nanoparticles [54], while nano-Se still needs further assessment. These nanoparticles promote wheat growth by activating the IAA signaling pathway [52].

The responses of salt-affected wheat cultivars to different concentrations of nano-Se are reflected in the improvement of wheat's vegetative parameters. Habibi and Aleyas (2020) [55] showed that shoot growth in barley was adversely affected by salinity concentrations up to 100 mM, while this drop was mitigated by the application of Se nanoparticles. Additionally, Domokos-Szabolcsy et al. (2012) [56] reported that treatment with Se-NPs (265–530 μ M) motivated the growth of the root system in tobacco (*Nicotiana tabacum*) grown by tissue culture. The results suggest that the application of Se nanoparticles has a positive effect against salinity in wheat plants. This study presents promising economic solutions that can be added to the traditional solutions used to manage agricultural environments affected by salts. It is necessary to continue testing biosynthetic nano-selenium on more crop plants under different abiotic stresses in order to reach a full understanding of the mechanisms of its effects, and thus improve its utilization.

5. Conclusions

The biological production of Se-NPs using green sources, such as plant enzymes, phytochemicals or proteins, as agents of reduction was and still is one of the most widely accepted techniques compared to chemical or physical methods. These biological tools have many advantages, particularly in their production of non-toxic nanoparticles and their environmental safety. The current study was conducted to isolate some bacterial strains that can produce Se-NPs and grow under salinity stress. The biological production of nanoparticles has gained a lot of attention recently due to their safety of use and lower toxicity. The bio-synthesis of nano-Se could be achieved using several species of bacteria,

fungi, algae, and some higher plants. These Se nanoparticles have distinct features that are exploited in the medicine, pharmaceutical and agricultural sectors. Therefore, the sustenance and promotion of cultivated plants using Se-NPs has proven beneficial under stressful environmental conditions, particularly salt stress, as stated in many studies.

Author Contributions: Data curation, A.A.G.; formal analysis, A.A.G., S.E.-N. and H.E.-R.; funding acquisition, H.E.-R. and W.L.; investigation, S.E.-N.; methodology, A.A.G. and S.E.-N.; project administration, H.E.-R.; resources, H.E.-R. and W.L.; supervision, W.L. All authors have read and agreed to the published version of the manuscript.

Funding: This research received no external funding.

Institutional Review Board Statement: Not applicable.

Informed Consent Statement: Not applicable.

Data Availability Statement: Not applicable.

Acknowledgments: This work was financially supported by the National Natural Science Foundation of China (41977121, 42177016), and the Central Department of Mission, Egyptian Ministry of Higher Education (Mission 19/2020) for El-Ramady.

Conflicts of Interest: The authors declare no conflict of interest.

References

1. Gebre, S.H.; Sendeku, M.G. New frontiers in the biosynthesis of metal oxide nanoparticles and their environmental applications: An overview. *SN Appl. Sci.* **2019**, *1*, 928. [\[CrossRef\]](#)
2. Juárez-Maldonado, A.; Ortega-Ortiz, H.; Morales-Díaz, A.B.; González-Morales, S.; Morelos-Moreno, Á.; Cabrera-De la Fuente, M.; Sandoval-Rangel, A.; Cadenas-Pliego, G.; Benavides-Mendoza, A. Nanoparticles and Nanomaterials as Plant Biostimulants. *Int. J. Mol. Sci.* **2019**, *20*, 162. [\[CrossRef\]](#) [\[PubMed\]](#)
3. Prajitha, N.; Athira, S.S.; Mohanan, P.V. Bio-interactions and risks of engineered nanoparticles. *Environ. Res.* **2019**, *172*, 98–108. [\[CrossRef\]](#) [\[PubMed\]](#)
4. Karthik, L.A.V.; Kirthi, S.; Ranjan, V.M.S. *Biological Synthesis of Nanoparticles and Their Applications*, 1st ed.; CRC Press: Boca Raton, FL, USA, 2020.
5. Zhang, H.; Zhou, H.; Bai, J.; Li, Y.; Yang, J.; Ma, Q.; Yuanyuan, Q. Biosynthesis of selenium nanoparticles mediated by fungus *Mariannaea* sp. HJ and their characterization. *Colloids Surf. A Physicochem. Eng. Asp.* **2019**, *571*, 9–16. [\[CrossRef\]](#)
6. Rastogi, A.; Zivcak, M.; Sytar, O.; Kalaji, H.M.; He, X.; Mbarki, S.; Brestic, M. Impact of Metal and Metal Oxide Nanoparticles on Plant: A Critical Review. *Front. Chem.* **2017**, *5*, 78. [\[CrossRef\]](#)
7. Naseem, T.; Tayyiba, D. The role of some important metal oxide nanoparticles for wastewater and antibacterial applications: A review. *Environ. Chem. Ecotoxicol.* **2021**, *3*, 59–75. [\[CrossRef\]](#)
8. Khot, L.R.; Sankaran, S.; Maja, J.M.; Ehsani, R.; Schuster, E.W. Applications of nanomaterials in agricultural production and crop protection: A review. *Crop Prot.* **2012**, *35*, 64–70. [\[CrossRef\]](#)
9. Waris, A.; Din, M.; Ali, A.; Ali, M.; Afridi, S.; Baset, A.; Khan, A.U. A comprehensive review of green synthesis of copper oxide nanoparticles and their diverse biomedical applications. *Inorgan. Chem. Commun* **2021**, *123*, 1387–7003. [\[CrossRef\]](#)
10. Hosnedlova, B.; Kepinska, M.; Skalickova, S.; Fernandez, C.; Ruttkey-Nedecky, B.; Peng, Q.; Baron, M.; Melcova, M.; Opatrilova, R.; Zidkova, J.; et al. Nano-selenium and its nanomedicine applications: A critical review. *Int. J. Nanomed.* **2018**, *13*, 2107. [\[CrossRef\]](#)
11. Khurana, A.; Tekula, S.; Saifi, M.A.; Venkatesh, P.; Godugu, C. Therapeutic applications of selenium nanoparticles. *Biomed. Pharmacother.* **2019**, *111*, 802–812. [\[CrossRef\]](#)
12. Sharma, G.; Sharma, A.R.; Bhavesh, R.; Park, J.; Ganbold, B.; Nam, J.S.; Lee, S.S. Biomolecule-mediated synthesis of selenium nanoparticles using dried *Vitis vinifera* (raisin) extract. *Molecules* **2014**, *19*, 2761–2770. [\[CrossRef\]](#)
13. Shoeibi, S.; Mozdziak, P.; Golkar-Narenji, A. Biogenesis of Selenium Nanoparticles Using Green Chemistry. *Top. Curr. Chem.* **2017**, *375*, 88. [\[CrossRef\]](#)
14. Gunti, L.; Dass, R.S.; Kalagatur, N.K. Phytofabrication of Selenium Nanoparticles From *Emblca officinalis* Fruit Extract and Exploring Its Biopotential Applications: Antioxidant, Antimicrobial, and Biocompatibility. *Front. Microbiol.* **2019**, *10*, 931. [\[CrossRef\]](#)
15. Liang, X.; Perez, M.A.M.; Nwoko, K.C.; Egbers, P.; Feldmann, J.; Csetenyi, L.; Gadd, G.M. Fungal formation of selenium and tellurium nanoparticles. *Appl. Microbiol. Biotechnol.* **2019**, *103*, 7241–7259. [\[CrossRef\]](#)
16. Presentato, A.; Piacenza, E.; Anikovskiy, M.; Cappelletti, M.; Zannoni, D.; Turner, R.J. Biosynthesis of selenium-nanoparticles and -nanorods as a product of selenite bioconversion by the aerobic bacterium *Rhodococcus aetherivorans* BCP1. *New Biotechnol.* **2018**, *41*, 1–8. [\[CrossRef\]](#)

17. Kumar, A.; Prasad, K.S. Role of nano-selenium in health and environment. *J. Biotechnol.* **2021**, *325*, 152–163. [[CrossRef](#)]
18. Tan, V.L.C.; Hinchman, A.; Williams, R.; Tran, P.A.; Fox, K. Nanostructured biomedical selenium at the biological interface (Review). *Biointerphases* **2018**, *13*, 06D301. [[CrossRef](#)]
19. Maiyo, F.; Singh, M. Selenium nanoparticles: Potential in cancer gene and drug delivery. *Nanomedicine* **2017**, *12*, 1075–1089. [[CrossRef](#)]
20. Maiyo, F.; Singh, M. Folate-Targeted mRNA Delivery Using Chitosan-Functionalized Selenium Nanoparticles: Potential in Cancer Immunotherapy. *Pharmaceuticals* **2019**, *12*, 164. [[CrossRef](#)]
21. Wang, X.; Pan, X.; Gadd, G.M. Immobilization of elemental mercury by biogenic Se nanoparticles in soils of varying salinity. *Sci. Total Environ.* **2019**, *668*, 303–309. [[CrossRef](#)]
22. Wang, X.; Zhang, D.; Pan, X.; Lee, D.J.; Al-Misned, F.A.; Mortuza, M.G.; Gadd, G.M. Aerobic and anaerobic biosynthesis of nano-selenium for remediation of mercury contaminated soil. *Chemosphere* **2017**, *170*, 266–273. [[CrossRef](#)]
23. Wadhvani, S.A.; Shedbalkar, U.U.; Singh, R.; Chopade, B.A. Biosynthesis of gold and selenium nanoparticles by purified protein from *Acinetobacter* sp. SW 30. *Enzyme Microb. Technol.* **2018**, *111*, 81–86. [[CrossRef](#)]
24. Shoeibi, S.; Mashreghi, M. Biosynthesis of selenium nanoparticles using *Enterococcus faecalis* and evaluation of their antibacterial activities. *J. Trace Elem. Med. Biol.* **2017**, *39*, 135–139. [[CrossRef](#)]
25. Fernández-Llamas, H.; Castro, L.; Blázquez, M.L.; Díaz, E.; Carmona, M. Biosynthesis of selenium nanoparticles by *Azoarcus* sp. CIB. *Microb. Cell Fact.* **2016**, *15*, 109. [[CrossRef](#)]
26. Cremonini, E.; Boaretti, M.; Vandecandelaere, I.; Zonaro, E.; Coenye, T.; Lleo, M.M.; Lampis, S.; Vallini, G. Biogenic selenium nanoparticles synthesized by *Stenotrophomonas maltophilia* SeITE02 loose antibacterial and antibiofilm efficacy as a result of the progressive alteration of their organic coating layer. *Microb. Biotechnol.* **2018**, *11*, 1037–1047. [[CrossRef](#)]
27. Tugarova, A.V.; Mamchenkova, P.V.; Dyatlova, Y.A.; Kamnev, A.A. FTIR and Raman spectroscopic studies of selenium nanoparticles synthesised by the bacterium *Azospirillum thiophilum*. *Spectrochim. Acta A Mol. Biomol. Spectrosc.* **2018**, *192*, 458–463. [[CrossRef](#)]
28. Cruz, D.M.; Mi, G.; Webster, T.J. Synthesis and characterization of biogenic selenium nanoparticles with antimicrobial properties made by *Staphylococcus aureus*, methicillin-resistant *Staphylococcus aureus* (MRSA), *Escherichia coli*, and *Pseudomonas aeruginosa*. *J. Biomed Mater. Res.* **2018**, *106*, 1400–1412. [[CrossRef](#)]
29. Kora, A.J.; Sashidhar, R.B. Biogenic silver nanoparticles synthesized with rhamnogalacturonan gum: Antibacterial activity, cytotoxicity and its mode of action. *Arab. J. Chem.* **2018**, *11*, 313–323. [[CrossRef](#)]
30. Penfield, S. Seed dormancy and germination. *Curr. Biol.* **2017**, *27*, R874–R878. [[CrossRef](#)]
31. Diaz-Mendoza, M.; Diaz, I.; Martinez, M. Insights on the Proteases Involved in Barley and Wheat Grain Germination. *Int. J. Mol. Sci.* **2019**, *20*, 2087. [[CrossRef](#)]
32. Guo, G.; Liu, X.; Sun, F.; Cao, J.; Huo, N.; Wuda, B.; Xin, M.; Hu, Z.; Du, J.; Xia, R.; et al. Wheat miR9678 Affects Seed Germination by Generating Phased siRNAs and Modulating Abscisic Acid/Gibberellin Signaling. *Plant Cell.* **2018**, *30*, 796–814. [[CrossRef](#)] [[PubMed](#)]
33. Ishibashi, Y.; Yuasa, T.; Iwaya-Inoue, M. Mechanisms of Maturation and Germination in Crop Seeds Exposed to Environmental Stresses with a Focus on Nutrients, Water Status, and Reactive Oxygen Species. *Adv. Exp. Med. Biol.* **2018**, *1081*, 233–257. [[CrossRef](#)] [[PubMed](#)]
34. Elkelish, A.A.; Soliman, M.H.; Alhaithloul, H.A.; El-Esawi, M.A. Selenium Protects Wheat Seedlings against Salt Stress-Mediated Oxidative Damage by Up-Regulating Antioxidants and Osmolytes Metabolism. *Plant Physiol. Biochem.* **2019**, *137*, 144–153. [[CrossRef](#)] [[PubMed](#)]
35. Feghhenabi, F.; Hadi, H.; Khodaverdiloo, H.; Van Genuchten, M. Seed priming alleviated salinity stress during germination and emergence of wheat (*Triticum aestivum* L.). *Agric. Water Manag.* **2020**, *231*, 106022. [[CrossRef](#)]
36. Alsaeedi, A.; El-Ramady, H.; Alshaal, T.; El-Garawani, M.; Elhawat, N.; Al-Otaibi, A. Exogenous nanosilica improves germination and growth of cucumber by maintaining K⁺/Na⁺ ratio under elevated Na⁺ stress. *Plant Physiol. Biochem.* **2018**, *125*, 164–171. [[CrossRef](#)]
37. Alsaeedi, A.H.; El-Ramady, H.; Alshaal, T.; El-Garawani, M.; Elhawat, N.; Almohsen, M. Engineered silica nanoparticles alleviate the detrimental effects of Na⁺ stress on germination and growth of common bean (*Phaseolus vulgaris*). *Environ. Sci. Pollut. Res. Int.* **2017**, *24*, 21917–21928. [[CrossRef](#)]
38. Ivani, R.; Sanaei Nejad, S.H.; Ghahraman, B.; Astarai, A.R.; Feizi, H. Role of bulk and Nanosized SiO₂ to overcome salt stress during Fenugreek germination (*Trigonella foenum-graceum* L.). *Plant Signal Behav.* **2018**, *13*, e1044190. [[CrossRef](#)]
39. Djanaguiraman, M.; Belliraj, N.; Bossmann, S.H.; Prasad, P.V.V. High-Temperature Stress Alleviation by Selenium Nanoparticle Treatment in Grain Sorghum. *ACS Omega.* **2018**, *3*, 2479–2491. [[CrossRef](#)]
40. Dimkpa, C.O.; Singh, U.; Bindraban, P.S.; Elmer, W.H.; Gardea-Torresdey, J.L.; White, J.C. Zinc oxide nanoparticles alleviate drought-induced alterations in sorghum performance, nutrient acquisition, and grain fortification. *Sci. Total Environ.* **2019**, *688*, 926–934. [[CrossRef](#)]
41. Hu, T.; Li, H.; Li, J.; Zhao, G.; Wu, W.; Liu, L.; Wang, Q.; Guo, Y. Absorption and Bio-Transformation of Selenium Nanoparticles by Wheat Seedlings (*Triticum aestivum* L.). *Front. Plant Sci.* **2018**, *9*, 597. [[CrossRef](#)]
42. Focht, D.D. Microbiological procedures for biodegradation research. *Methods Soil Anal. Part 2 Microbiol. Biochem. Prop.* **1994**, *5*, 407–426.

43. Krieg, N.R.; Manual, H.J.C.B. *Systematic Bacteriology*; Williams: Baltimore, MD, USA, 1984.
44. Ranal, M.A.; Santana, D.G. How and why to measure the germination process? *Rev. Bras. Bot.* **2006**, *29*, 1–11. [[CrossRef](#)]
45. Mauromicale, G.; Licandro, P. Salinity and temperature effects on germination, emergence and seedling growth of globe artichoke. *Agronomie* **2002**, *22*, 443–450. [[CrossRef](#)]
46. Kharb, R.P.S.; Lather, B.P.S.; Deswal, D.P. Prediction of field emergence through heritability and genetic advance of vigour parameters. *Seed Sci. Technol.* **1994**, *22*, 461–466.
47. Esehie, H.A. Interaction of Salinity and Temperature on the Germination of Sorghum. *J. Agron. Crop Sci.* **1994**, *172*, 194–199. [[CrossRef](#)]
48. Vincent, J.M. *A Manual for the Practical Study of the Root- Nodule Bacteria*; IBP Handbook No. 15.; Blackwell Scientific Publications Oxford and Edinburgh: Oxford, UK; Edinburgh, UK, 1970; pp. 54–58.
49. Duncan, B.D. Multiple ranges and multiple F. test. *Biometrics* **1955**, *11*, 1–42. [[CrossRef](#)]
50. Sathishkumar, M.; Sneha, K.; Won, S.W.; Cho, C.-W.; Kim, S.; Yun, Y.-S. Cinnamon zeylanicum bark extract and powder mediated green synthesis of nano-crystalline silver particles and its bactericidal activity. *Colloids Surfaces B Biointerfaces* **2009**, *73*, 332–338. [[CrossRef](#)]
51. Liu, D.; Han, C.; Deng, X.; Liu, Y.; Liu, N.; Yan, Y. Integrated Physiological and Proteomic Analysis of Embryo and Endosperm Reveals Central Salt Stress Response Proteins During Seed Germination of Winter Wheat Cultivar Zhengmai 366. *BMC Plant Biol.* **2019**, *19*, 29. [[CrossRef](#)]
52. Li, R.; He, J.; Xie, H.; Wang, W.; Bose, S.K.; Sun, Y.; Hu, J.; Yin, H. Effects of chitosan nanoparticles on seed germination and seedling growth of wheat (*Triticum aestivum* L.). *Int. J. Biol. Macromol.* **2019**, *126*, 91–100. [[CrossRef](#)]
53. Du, W.; Yang, Y.; Peng, Q.; Liang, X.; Mao, H. Comparison Study of Zinc Nanoparticles and Zinc Sulphate on Wheat Growth: From Toxicity and Zinc Biofortification. *Chemosphere* **2019**, *227*, 109–116. [[CrossRef](#)]
54. Sundaria, N.; Singh, M.; Upreti, P.; Chauhan, R.P.; Jaiswal, J.P.; Kumar, A. Seed Priming with Iron Oxide Nanoparticles Triggers Iron Acquisition and Biofortification in Wheat (*Triticum aestivum* L.) Grains. *J. Plant Growth Regul.* **2019**, *38*, 122–131. [[CrossRef](#)]
55. Habibi, G.; Aleyasin, Y. Green synthesis of Se nanoparticles and its effect on salt tolerance of barley plants. *Int. J. Nano Dimens.* **2020**, *11*, 145–157.
56. Domokos-Szabolcsy, E.; Marton, L.; Sztrik, A.; Babka, B.; Prokisch, J.; Fari, M. Accumulation of red elemental selenium nanoparticles and their biological effects in *Nicotiana tabacum*. *Plant Growth Regul.* **2012**, *68*, 525–531. [[CrossRef](#)]